COMPUTATIONAL HIGH-FREQUENCY WAVE PROPAGATION USING THE LEVEL SET METHOD, WITH APPLICATIONS TO THE SEMI-CLASSICAL LIMIT OF SCHRÖDINGER EQUATIONS

LI-TIEN CHENG, HAILIANG LIU, AND STANLEY OSHER

Abstract. We introduce a level set method for computational high frequency wave propagation in dispersive media and consider the application to linear Schroödinger equations with high frequency initial data. High frequency asymptotics of dispersive equations often lead to the well-known WKB system where the phase of the plane wave evolves according to a nonlinear Hamilton-Jacobi equation and the intensity is governed by a linear conservation law. From the Hamilton-Jacobi equation, wave fronts with multiple phases are constructed by solving a linear Liouville equation of a vector valued level set function in the phase space. The multi-valued phase itself can be constructed either from an additional linear hyperbolic equation in phase space or an additional linear homogeneous equation and component to the level set function in an augmented phase space. This phase is in fact valid in the entire physical domain, but one of the components of the level set function can be used to restrict it to a wave front of interest. The use of the level set method in this numerical approach provides an Eulerian framework that automatically resolves the multi-valued wave fronts and phase from the superposition of solutions of the equations in phase space.

Key Words: Level set method, Schrödinger's equation, semiclassical limit, wave front, multi-valued phases

AMS subject classification: Primary 35Q55; Secondary 65M25

Contents

1. Introduction

In this work, we are interested in the computation of high frequency propagating waves for equations arising in dispersive media. The intention of this paper is to introduce a general level set method and framework for multi-phase computations of problems of this type. However, the application that we focus on is the time-dependent multi-dimensional

Schrödinger equation,

$$i\epsilon\partial_t\psi^\epsilon = -\frac{\epsilon^2}{2}\Delta\psi^\epsilon + V(x)\psi^\epsilon, \quad x \in \mathbb{R}^n, \tag{1.1}$$

subject to the high frequency initial data,

$$\psi^\epsilon(x,0) = A_0(x)\exp\left(i\frac{S_0(x)}{\epsilon}\right), \tag{1.2}$$

where ψ^ϵ is the complex wave field, $V(x)$ is a given potential function, and $\epsilon > 0$, appearing in both the equation and the initial data, denotes a re-scaled Planck constant. Here the regime of interest is the so-called *semiclassical regime*, where ϵ tends to zero.

Apart from quantum mechanics, problem (1.1) with (1.2) arises in many contexts in classical wave propagation such as the paraxial approximation of forward propagating waves [26]. Thus, it is of practical importance for computing high frequency wave propagations in many applied fields such as radio engineering [27], laser optics [59], underwater acoustics [60], the investigation of light and sound propagation in turbulent atmosphere [61], seismic wave propagation in the Earth's crust [54], Bose Einstein condensates [1], and a host of other subjects. In these applications, the potential V is explicitly related to the feature of the propagating medium.

In the semiclassical regime, where the scaled Planck constant ϵ is small, one can seek plane wave solutions with the WKB ansatz,

$$\psi^\epsilon = A^\epsilon(x,t)\exp(iS(x,t)/\epsilon).$$

Assuming that the phase S and the amplitude A^ϵ are sufficiently smooth, we may expand the amplitude in powers of ϵ,

$$A^\epsilon = A_0 + \epsilon A_1 + \epsilon^2 A_2 + \cdots.$$

Inserting this expression into (1.1) and balancing terms of $O(1)$ order in ϵ with separate real and imaginary parts leads to separate equations for A and S. The phase function S will satisfy a nonlinear first order equation of Hamilton-Jacobi type,

$$\partial_t S + H(x,\nabla S) = 0, \quad H(x,p) := V(x) + |p|^2/2, \tag{1.3}$$

and the amplitude A_0 solves a transport equation,

$$\partial_t A_0^2 + \nabla\cdot(A_0^2\nabla S) = 0. \tag{1.4}$$

When ϵ is small, the leading term, A_0, becomes significant. The above system is weakly coupled since the phase S can be solved independently from equation (1.3). This Hamilton-Jacobi equation in general develops a singularity in finite time. A standard numerical method using the analogue of shock capturing ideas for the Hamilton-Jacobi equation will select a unique solution, called the viscosity solution [17, 43]. Unfortunately, this class of weak solutions is not appropriate for treating dispersive wave propagation problems. As is known in the literature, see, e.g., [9, 19, 11, 12, 31, 55], using the entropy notion for the eikonal equation leads to a measure-valued solution, i.e., solution of delta function type, in the intensity A^2 on the shock curves of the phase. These singularities are called caustics since the energy of the wave becomes infinite there. This clearly contradicts the a priori estimates for (1.1). A natural way to avoid such difficulties is to seek multi-valued phases corresponding to crossing waves. This means in general, for every fixed (x,t) which is not on the caustic, one tries to construct a set of phase functions $\{S_i\}$, $i = 1, 2, \cdots$, each

of which is a solution of the Hamilton-Jacobi equation in a neighborhood of (x,t). This set is referred to as the multi-valued solution of the Hamilton-Jacobi equation. Actually in the context of wave propagation, the correct solution generally allows a multi-valued phase while the viscosity solution picks out the phase corresponding to the first arrival wave.

Given multi-valued phase functions, uniform asymptotic formulas for the wave field near the caustics can be constructed via several techniques such as boundary layer techniques [2, 10] as well as phase space approaches, Lagrangian integrals [18, 41, 42], and the method of canonical operator [44, 63].

A relatively new phase space technique for studying oscillatory solutions of dispersive equations is based on the use of the Wigner transform, which has drawn increasing interest, see e.g., [3, 29, 34, 37, 39, 56]. The Wigner transformation provides a phase space description of the equations of the problem and has been shown to be very useful for asymptotics since it "unfolds" the caustics, due to the linearity of the Liouville equation used in the phase space. This technique provides an alterative approach to the WKB method, see, e.g., [56]. There is, however, a serious drawback in the direct numerical approximation of the Liouville equation. There are two ways to remedy this problem in the literature. One is the moment method which is based on reducing the number of independent variables by introducing equations for moments. The other is based on computations of special wave front solutions. For tracking wave fronts in geometrical optics, some geometry based methods in phase space such as the segment projection method [23] and level set method [47, 15, 52] have been recently introduced. Consult [21] for a recent survey on computational high frequency wave propagation in geometrical optics.

In this paper we introduce a general level set method for computing multi-valued solutions to more general HJ equations of the form (1.3), which includes the one studied in [47]. Computation of the multi-valued density based on (1.4) is left to a future work. We begin by sketching the idea explored in the present work. A formal analysis of the HJ equation (1.3), obtained by tracking classical characteristics, suggests that a solution will in general become multi-valued in finite time. The bi-characteristics in (x,p) space, governed by (2.2)-(2.3), may be referred to as rays, as in geometrical optics [47]. It is shown that in general the phase S changes its shape along the ray in (x,p) space and in fact satisfies a forced hyperbolic transport equation,

$$\partial_t S + F\cdot\nabla_{\{x,p\}}S = B, \quad F := (\nabla_p H, -\nabla_x H)^\top, \quad B = p\cdot\nabla_p H - H. \tag{1.5}$$

The linearity of this equation "unfolds" the caustics in the phase space of $(x,p)\in \mathbb{R}^{2n}$, but the equation itself is not enough for us to resolve the multi-valued phase S in physical space. In order to do so we need to restrict the phase value to the manifold $p=\nabla_x S$ in (x,p) space and then project to the physical space of $x\in\mathbb{R}^n$. Our approach to identify the manifold $p=\nabla_x S$ is by the intersection of the zero level sets of n functions in (x,p) space. These level set functions, labeled $\phi=\phi(t,x,p)$ in general, evolve according to the linear homogeneous equation,

$$\partial_t\phi + \nabla_p H\cdot\nabla_x\phi - \nabla_x H\cdot\nabla_p\phi = 0 \tag{1.6}$$

with proper chosen initial data, e.g., ϕ_0 a component of $p-\nabla_x S_0$. This equation has the advantage of the linear superposition property of the ray equations and, like the HJ equation, the solution is defined by PDE's and can easily be computed on a uniform

Eulerian grid. Note also that this equation has the same form as the Liouville equation encountered in kinetic model based methods except that the solution here is the level set function, instead of a particle density function. With this in mind we still call it a Liouville equation.

In order for our approach to be applied to more general cases and if we wish to place the computation of multi-valued S in the level set framework, we may look at the graph of the phase $z = S(x, p, t)$ in $\mathbb{R}^{2n+1}$. This translates to the addition of a level set function, still labeled $\phi = \phi(t, x, p, z)$, in the augmented phase space $(x, p, z) \in \mathbb{R}^{2n+1}$. Evolution of this function is under the equation

$$\partial_t \phi + F \cdot \nabla_{\{x,p\}} \phi + B \partial_z \phi = 0, \tag{1.7}$$

where the initial data can be taken to be $\phi_0 = z - S_0(x)$. In this way, the multi-valued S on the whole physical domain can be obtained from the intersection of the zero level sets of the $n+1$ level set functions in (x, p, z) which evolve under n equations of the form (1.6) and the equation (1.7).

In order to gain further insight into the structure of the multi-valued solution S, we are also interested in computing the wave front solution, i.e., some special solution associated with the underlying front surface. Note that in the context of geometrical optics, as studied in [47], the phase does not change its shape along the ray. The wave front is therefore defined as the level curve of the phase and the wave front solution is completely determined by computing the front location. However in the current Schrödinger setting the phase S does change its shape along the ray in (x, p) space. The natural question is in what sense is the wave front defined? Consistent with the geometrical optics case, in this paper we define the wave front, or more specifically, bicharacteristic strips, to be the $n-1$ dimensional surface in (x, p) space, driven by the Hamiltonian dynamics (2.2)-(2.3), and starting with a level surface of the initial phase S_0. For the computation of such a defined wave front solution, we need to add a level set function and an evolution equation for it. The location of our defined front surface can be tracked, as in [47], by the intersection of the zero level sets of $n+1$ level set functions in (x, p) space evolving according to (1.6). n of these functions can be initialized as the components of $p - \nabla_x S_0$, as before, and the one remaining function can be initialized as the level set of interest of the initial phase, e.g., $S_0(x) - C$.

In summary using the above two general level set equations, multi-valued phase in the whole physical domain is resolved and multi-valued wave fronts are tracked via the intersection of zero level sets of several level set functions. Note that in the above procedures we always need the n level set equations initialized to the components of $p = \nabla_x S$. This is not surprising since the Hamiltonian is nonlinear in p. The intersection of these n level set equations actually gives an approximate phase gradient for the HJ equation. It would be interesting to clarify how faithful the computed multi-valued gradient $\nabla_x S$ is.

We wish to point out that the "graph" idea used here is not new and is already extensively explored in various contexts, see, e.g. [16, 24, 46, 62]. However the idea of building the "graph" and the "gradient" into level set functions that satisfy linear homogeneous PDE's is new and very general. With this idea we have recently developed a new level set framework for tracking multi-valued solutions for a general class of nonlinear first-order equations [40] which include quasilinear hyperbolic transport equations and nonlinear Hamilton-Jacobi equations as two prototypical examples in this category. The level set

equations we obtained in this context are indeed consistent with classical characteristic theory [16] in the sense that the level set function evolves with the characteristic speed given by the theory. If the Hamiltonian is linear in p, it is not necessary to include the gradient in the level set formulation for S, thus reducing the case to the one given in [16] for a scalar quasilinear transport equation.

We note that [38] have subsequently but independently derived the same level set Liouville equations for the gradient of phase through an approach involving the techniques of [16] and [62]. The technique they adopt can in addition be used to obtain multi-valued solutions of scalar quasilinear hyperbolic equations. For Hamilton-Jacobi equations, the multi-valued gradient of the solution is derived.

In the calculation of wave propagation, high frequency approximations have been extensively used and proved to be quite accurate both numerically and analytically. In such an approach, phase and amplitude vary on a much slower scale than the wave field in the original wave equations and are thus easier to compute. However, such approximations fail either on caustics and focal points, where they predict wave amplitudes, or in shadow regions (i.e., regions devoid of rays), where they yield zero fields. On the other hand, the formation of caustics is a typical situation in many physical systems, for example, in seismology as a result of multiphase propagation from localized sources. From the mathematical point of view, the formation of caustics and the related multi-valuedness of the phase function is the main obstacle in constructing global high frequency solutions of the dispersive wave equation.

In this context the main numerical issue is to compute the multi-valued solution of the Hamilton-Jacobi equation in order to capture the multiple phases in the wave propagation. For this a number of numerical techniques have been proposed, see, e.g., [4, 5, 20, 22, 53]. For multi-phase computations in the semiclassical limit of the Schrödinger equation, see, e.g. [32, 37]. Our main goal in this paper is, again, to formulate a generic level set framework to compute the multi-valued solutions of the above Hamilton-Jacobi equations and to track the wave fronts and associated phases.

The problem of numerically obtaining multiple phases in geometrical optics has traditionally been handled by solving the characteristic field related to the eikonal equation. This involves ray tracing methods using the linear superposition principle and can be formulated, in the Lagrangian view point, as solving a system of ODE's to track the wave front. An obvious drawback of this method lies in obtaining adequate spatial resolution of the wave front in regions with diverging rays. Recently, the multi-valued phase function has been handled by properly partitioning the propagation domain and using eikonal solvers (see, e.g., [20]). A different approach is based on the kinetic formulation in phase space, in terms of a density function that satisfies Liouville's equation, where the technique used to capture the multi-valued solutions is based on a closure assumption of a system of equations for the moments of the density, as remarked earlier, see, e.g., [6, 7, 22, 30, 32, 33, 37, 53].

Before closing this section, we would like to point out the similarities and differences of the Wigner transform approach and the level set approach we employ in this work. Our interest via the level set method is to track the wave front with multi-phases and compute the multi-valued solution S in the whole domain. For the Hamilton-Jacobi equation for phase S, we choose the zero level set to be the wave front of the phase and track its evolution by solving a level set equation, i.e., the Liouville equation (1.6) in the phase

space (x,p). As remarked earlier we resolve the phase S by evolving a zero level set in an extended space (x,p,z) via the level set equation (1.7). Since the phase does not stay on any zero level set in (x,p) space, it satisfies the forced hyperbolic equation,

$$\partial_t S + (p, -\nabla_x V)^\top \cdot \nabla_{x,p} S = |p|^2/2 - V(x).$$

In the Wigner approach, the Wigner transform of the wave field is defined by

$$W^\epsilon(x,k,t) := \frac{1}{2\pi}\int_{-\infty}^{\infty} exp(-iky)\psi^\epsilon(x+\frac{\epsilon y}{2},t)\bar{\psi}^\epsilon(x-\frac{\epsilon y}{2},t)dy.$$

The most natural candidate for the solution of the Wigner equation is the Wigner transform of the WKB solution $\psi^\epsilon = A(x,t)exp(iS(x,t)/\epsilon)$, which reads,

$$W^\epsilon(x,k,t) = \frac{1}{\pi\epsilon}\int A(x+y,t)A(x-y,t)exp(iF(y;x,k,t)/\epsilon)dy,$$

where the Wigner phase F is given by

$$F = S(x+y,t) - S(x-y,t) - 2ky.$$

The main contribution of this integral comes from the stationary point of the phase F, i.e., $\partial_y F = 0$, which relates the kinetic speed to the phase gradient around the Lagrangian manifold $\{(x,k)|k = \nabla_x S\}$, i.e.,

$$k = \frac{\nabla_x S(x+y) + \nabla_x S(x-y)}{2},$$

and the weak limit of this Wigner integral becomes $|A(x)|^2\delta(k - \nabla_x S(x))$, see, e.g., [25]. After the Wigner function is computed, the position density $|\psi|^2$ and the momentum $|\phi|^2\nabla_x S$ are recovered via the moment procedure, see, e.g., [37]. It is interesting to see that both Wigner function and the level set function we consider in (x,p) space both satisfy the *Liouville equation* of the same form (1.6) even though the phase speed in both cases calls for a different interpretation.

This paper is organized as follows: §2 is devoted to formulating a new level set equation for which the switch from Lagrangian coordinates to Eulerian formulation is described. In §3 we discuss the possible reduction of the phase space dimension and explain the possible failure of such a reduction in some cases. §4 is devoted to documenting the numerical techniques used in our level set approach in a multi-dimensional setting; In §5 we present a selected group of numerical simulations.

The main observation and results in this paper were reported in detail by the first author at several occasions including the IPAM Lake Arrowhead Reunion Workshop, September 15-19, 2002; Princeton University, September 30, 2002, CSCAMM in the University of Maryland, December 3, 2002, and the IPAM workshop on "Emerging Applications of Nonlinear Schrödinger equations", Feb 6-10, 2003. For slides see [14].

2. Level Set Formulation

The level set method is a computational method for tracking the evolution of interfaces, proposed in [49]. The idea is to represent a curve/surface as a zero level set of some properly chosen function. The motion of the curve/surface is given by a transport equation based on the physics describing the evolution of the interface.

The choice of the level set function depends on the interface considered. In the context of the semiclassical regime, we are interested in both wave front propagation and the phase determined by Schrödinger's equation.

We proceed in two steps to realize the phase value S via the level set method.

Step 1. Evolution in phase space, $(x,p) \in \mathbb{R}^{2n}$,

The solution S of the Hamilton-Jacobi equation,

$$\partial_t S + H(x, \nabla_x S) = 0, \tag{2.1}$$

can be obtained, at least locally, by the method of characteristics. This means that each point in the neighborhood of the initial manifold is reached by a unique integral curve $x(t,\alpha)$, called a ray, with $x(\alpha,0)=\alpha$ being the initial position of each ray. Set

$$p := \nabla_y S(x(t,\alpha),t),$$

the curves, $(t,\alpha) \to (x(t,\alpha), p(t,\alpha))$, called bicharacteristics, and solve the ODE's

$$\frac{dx}{dt} = \nabla_p H(x,p), \quad x(0,\alpha)=\alpha, \tag{2.2}$$

$$\frac{dp}{dt} = -\nabla_x H(x,p), \quad p(0,\alpha) = \nabla_x S_0(\alpha). \tag{2.3}$$

Having solved this system we obtain the solution of the HJ equation (2.1) by integrating

$$\frac{dS(x,t)}{dt} = p\cdot\nabla_p H(x,p) - H(x,p), \quad S(x(0,\alpha),0) = S_0(\alpha). \tag{2.4}$$

Let the initial manifold be parameterized as $\{\alpha = \gamma(\theta), \quad \theta \in I \subset \mathbb{R}\}$ and let $p_0(\theta)$ and $S_0(\theta)$ be given functions on the initial manifold. The projection $\{x = x(t,\theta), \quad t \in \mathbb{R}^+, \theta \in I\}$ of the characteristics onto R^n are the usual rays of geometrical optics. The solution of the Hamilton-Jacobi equation is given by

$$S(x(t,\theta),t) = S_0(\gamma(\theta)) + \int_0^t (p\cdot\nabla_p H - H)dt,$$

where the integral is calculated along the characteristics.

The transformation

$$(t,\theta) \to x(t,\theta)$$

is invertible and (t,θ) may be non-smooth or multi-valued functions of x. Thus rays may intersect but the characteristics will never intersect in phase space. The phase solution $S(x,t)$ may also be a multi-valued function.

To allow the multi-valued description of the phase $S(x,t) = \{S_i(x,t)\}_{i=1}^N$, we study the evolution of S in the phase space of $(x,p) \in \mathbb{R}^{2n}$, governed by

$$\partial_t S + \nabla_p H(x,p)\cdot\nabla_x S - \nabla_x H(x,p)\cdot\nabla_p S = p\cdot\nabla_p H(x,p) - H(x,p). \tag{2.5}$$

Since this equation is linear we know that the solution S exists for all time. In contrast to the case of a nonlinear HJ equation (2.1), we have global solutions for (2.5), i.e., no caustics appear in phase space! Note that the initial data is given by $p = \nabla_x S_0(\alpha)$ and the curves $x(t,\alpha)$ are the rays associated to the Hamilton-Jacobi equation (2.1) with initial

data $S(x,0) = S_0(\alpha)$. This reflects the fact that the bicharacteristics in phase space are projected down to rays $x(t,\alpha)$ in physical space and include an additional curve $p(t,\alpha)$, which is the gradient of the phase S along the rays.

Clearly the phase S does not stay on any zero level set in (x,p) space since it satisfies a forced hyperbolic transport equation (2.5). To evolve S as a whole solution to (2.1) via a zero level set, one can extend the phase space by introducing an additional variable.

Step 2. The choice of the level set function

The wave front to be tracked can be realized as the intersection of the zero level sets of $n+1$ level set functions as described previously. Each level set function remains unchanged along the characteristics, which implies that each level set function ϕ solves the *Liouville equation*

$$\partial_t \phi + U \cdot \nabla \phi = 0 \tag{2.6}$$

with velocity field $U = (\nabla_p H, -\nabla_x H)$. Among the $n+1$ level set functions, n are used to represent $p = \nabla_x S$ and one is used to identify the front location.

The choice of the level set for realizing the multi-valued phase S depends on the specific form of the Hamiltonian $H(x,p)$.

1) If $H(x,p)$ is homogeneous of degree 1 in p, i.e., for any $\lambda \in \mathsf{IR}^+$, $H(x,\lambda p) = \lambda H(x,p)$, then $p \cdot \nabla_p H = H$, and thus S satisfies the homogeneous equation

$$\partial_t S + \nabla_p H(x,p) \cdot \nabla_x S - \nabla_x H(x,p) \cdot \nabla_p S = 0, \tag{2.7}$$

which implies that S remains constant along the ray. One can simply solve this homogeneous hyperbolic PDE, the same as the Liouville equation (2.6) above, since its linearity already "unfolds" the possible multi-valuedness in (x,p) space. For the wave front solution one just needs to locate the multi-valued front surface as above, see [47], since S remains the same on the wave front surface. The multi-valued S on the physical domain, which was not computed in [47], is simply the restriction of S, obtained by solving 2.7 directly with initial data $S_0(x)$, on the manifold $p = \nabla_x S$, which is obtained by the intersection of the first n zero level sets stated above.

A prototypical example is the geometrical optics approximation for the wave equation

$$\partial_t^2 u = c(x)\Delta u,$$

for which the phase satisfies

$$\partial_t S + c(x)|\nabla_x S| = 0,$$

which is the HJ equation (1.3) with $H = c(x)|p|$, see [22, 23, 47].

2) For a general Hamiltonian $H(x,p)$, the source term $p\cdot\nabla_p H - H$ may not be identically zero. The phase of the wave function will change its shape along the rays. The level set method in [47] does not work in this case even for computing the multi-valued wave front solution. Thus we derive here a new level set formulation for realizing S.

We introduce an artificial space variable z and consider the characteristic field (2.2)-(2.3) augmented with velocity field in z,

$$\frac{dz}{dt} = p \cdot \nabla H_p(x,p) - H(x,p).$$

Note that the above equation when combined with (2.4) implies that the graph $z = S(t,x,p)$ is preserved along the extended characteristics,

$$\begin{aligned}
&\frac{dx}{dt} = \nabla_p H(x,p), \quad x(0,\alpha) = \alpha,\\
&\frac{dp}{dt} = -\nabla_x H(x,p), \quad p(0,\alpha) = \nabla_x S_0(\alpha),\\
&\frac{dz}{dt} = p \cdot \nabla H_p(x,p) - H(x,p), \quad z(0,\alpha) = S_0(\alpha).
\end{aligned}$$

We introduce a level set function $\phi = \phi(t,x,p,z)$ so that the graph $z = S$ can be realized as a zero level set,

$$\phi(t,x,p,z) = 0, \quad z = S(t,x,p). \tag{2.8}$$

This level set function should also be preserved along the extended characteristics, i.e., it solves the transport equation

$$\partial_t \phi + U \cdot \nabla_{\{x,p,z\}} \phi = 0, \tag{2.9}$$

where the corresponding velocity field is

$$U = (\nabla_p H, \quad -\nabla_x H, \quad p \cdot \nabla_p H - H).$$

In fact the above level set equation can also be formally derived from the hyperbolic PDE (2.5) in a similar manner as in [16, 62]. Taking the gradient of the zero level set (2.8), one has

$$\nabla_{\{t,x,p\}} \phi + \partial_z \phi \nabla_{\{t,x,p\}} S = 0, \tag{2.10}$$

where we have used the fact that $z = S(t,x,p)$. Note that $\partial_z \phi \neq 0$, so multiplication of (2.5) by $-\phi_z$ when combined with (2.10) leads to the above level set equation (2.9).

To realize S in (x,p) space one needs just one level set function, which can be generated by solving (2.9) with initial data simply chosen as

$$\phi(0,x,p,z) := z - S_0(x).$$

To resolve S in the physical space $x \in \mathsf{IR}^n$ one needs to also resolve p by an additional n level set functions, call them ϕ_i, which can be generated by solving the level set equation (2.9) with initial data chosen as

$$\phi_i(0,x,p,z) = p_i - \partial_{x_i} S_0(x), \quad i = 1 \cdots n.$$

Since both H and the initial data chosen in this way do not depend explicitly on S, the level set equation (2.9) reduces to the linear Liouville equation (2.6) without z involved. Geometrically the graph $z = S$ is realized by the intersection of a z related zero level set and n gradient-related zero level sets; the multi-valued front surface is tracked by the intersection of a front related zero level set and n gradient-related zero level sets. In both procedures the intersection of the latter n gradient-related zero level sets also approximately resolves $\nabla_x S$ in the whole physical domain.

Clearly in order to track wave fronts one can still work in (x,p) space and solve the linear *Liouville equation* (2.6). However using level set functions in the extended (x,p,z) space enables us to evolve the phase S as a zero level set in the entire physical domain.

3. Reduction of the Phase Space

In practice, one encounters problems with available computer memory when performing higher dimensional computations. This section is devoted to the possible reduction of the phase space dimension. We shall illustrate this with the case $x \in \mathbb{R}^2$. Higher dimensions can be handled in a similar manner.

Along the flow determined by the velocity field, $U = (\nabla_p H, -\nabla_x H)$,

$$\frac{d}{dt}H = U \cdot \nabla_{\{x,p\}} H = 0,$$

hence the energy is conserved,

$$H(x,p) = H(\alpha, p_0(\alpha)), \tag{3.1}$$

where α denotes the initial position of each particle path.

One of our goals is to visualize the propagation of the wave front for any given initial wave profile. Assume the initial level curve is determined by $\phi_0(x) = 0$, then

$$\alpha \in \{x, \quad \phi_0(x) = 0\}.$$

Let this level curve be parameterized in terms of a single quantity ψ. Then one has $\alpha = \alpha(\psi)$ and also $H(\alpha, p_0(\alpha)) = H_0(\psi)$. Since along the particle path this parameter does not change, we have

$$\frac{d}{dt}\psi = 0. \tag{3.2}$$

This technique was introduced in [35]. Since $H(x,p) = |p|^2/2 + V(x)$, the conservation of the energy (3.1) tells us that the amplitude of the ray $|p|$ can be expressed in terms of x and ψ, i.e.,

$$|p| = \sqrt{2(H_0(\psi) - V(x))}. \tag{3.3}$$

The above facts enable us to reduce the phase space from $(x,p,z) \in \mathbb{R}^5$ to $\mathbb{R}^4$.

Let $p = |p|(cos\theta, sin\theta)$ in polar coordinates with $\theta \in [-\pi, \pi]$. One then has

$$p' = |p|'(cos\theta, sin\theta) + |p|(-sin\theta, cos\theta)\theta'.$$

Multiplying this by $(-sin\theta, cos\theta)^\top$ on the right gives

$$\theta' = \frac{p'}{|p|} \cdot (-sin\theta, cos\theta)^\top.$$

Therefore from $H = \frac{|p|^2}{2} + V(x)$ it follows the velocity field is

$$\begin{aligned}
\frac{dx}{dt} &= \nabla_p H = p = |p|(cos\theta, sin\theta), \\
\frac{dp}{dt} &= -\nabla_x H = -\nabla V(x), \\
\frac{dz}{dt} &= p \cdot \nabla_p H - H = \frac{|p|^2}{2} - V(x) = H_0(\psi) - 2V(x).
\end{aligned}$$

This when combined with (3.3) leads to the reduced Lagrangian formulation for $\frac{d}{dt}(x,\theta,z) = U$ with velocity field

$$U_1 = \sqrt{2(H_0(\psi) - V(x))}cos\theta, \tag{3.4}$$

$$U_2 = \sqrt{2(H_0(\psi) - V(x))}sin\theta, \tag{3.5}$$

$$U_3 = \frac{V_{x_1}sin\theta - V_{x_2}cos\theta}{\sqrt{2(H_0(\psi) - V(x))}}, \tag{3.6}$$

$$U_4 = H_0(\psi) - 2V(x). \tag{3.7}$$

Therefore in the reduced phase space, $(x,\theta,z) \in \mathsf{IR}^4$, the level set equation (2.9) becomes

$$\partial_t\phi + U(x,\theta,\psi)\cdot\nabla_{\{x,\theta,z\}}\phi = 0, \quad (x,\theta,z) \in \mathsf{IR}^4.$$

This equation is not closed because the velocity depends on the Lagrangian index ψ, which is constant just along the flow. In the Eulerian formulation this Lagrangian index satisfies the same transport equation as the level set does, i.e.,

$$\partial_t\psi + U(x,\theta,\psi)\cdot\nabla_{\{x,\theta,z\}}\psi = 0.$$

We can use an upwind type scheme to solve this transport equation, even if it is very slightly nonlinear. The level set function evolves based on the updated velocity field.

The choice of ψ is not unique, however, one can take $\psi = H$ in the above setting since the energy H is conserved along the characteristics. Note, in fact, that ψ appears only in the term $H(\psi)$ and so, alternatively, we may track the value of H along with the wave front, using the value when needed for the velocity field.

From the velocity in the reduced space we observe that the singularity may appear for non-vanishing potential, and thus working in the full space is still necessary.

For $x \in \mathsf{IR}^1$ such reduction is unnecessary. In this case there is no wave front to be tracked, however the phase value in the whole space $x \in \mathsf{IR}^1$ can be easily realized via the intersection of two zero level sets

$$\phi_i(t,x,p,z) = 0, \quad i = 1,2,$$

where ϕ_1 is generated by solving the linear Liouville equation,

$$\partial_t\phi_1 + \partial_p H\partial_x\phi_1 - \partial_x H\partial_p\phi_1 = 0 \tag{3.8}$$

with initial data chosen as

$$\phi_1(0,x,p,z) = p - \partial_x S_0(x);$$

the level set function ϕ_2 is obtained by evolving the *generalized* Liouville equation,

$$\partial_t\phi_2 + \partial_p H\partial_x\phi_2 - \partial_x H\partial_p\phi_2 + (p\partial_p H - H)\partial_z\phi_2 = 0 \tag{3.9}$$

subject to initial data chosen as

$$\phi_2(0,x,p,z) = z - S_0(x).$$

4. Numerical Techniques

Our main task is two-fold: (1) construct the wave front and track its evolution; resolve the associated multi-valued phase. (2) resolve the multi-valued phase S in the entire domain.

As shown in Section 2, for (1), we need to compute $n+2$ level set functions, among which $n+1$ level set functions can be used to resolve the multi-valued phase S in the whole physical domain. In our numerical simulations we shall focus mainly on the 2-dimensional case. We thus compute the multi-valued wave front solution in (x, p) space by solving the Liouville equation (1.6), where the multi-valued S is obtained from solving the forced hyperbolic equation (2.5) and then extracting it on the obtained front surface. In the one-dimensional case, we illustrate (2) by the use of $n+1=2$ level set functions in (x, p, z) space by solving a coupled system (1.6) and (1.7). Consult [40] for the computation of multi-valued solutions of more general nonlinear first-order PDE's.

The numerical technique for wave front construction in the setting we describe here follows the framework and ideas of [47] for geometrical optics. Wave front construction in geometrical optics encounters many of the same difficulties, namely that of resolving wave fronts and handling multi-valued solutions. The approach taken in the recent works of [23, 28, 47] is to work in phase space on bicharacteristic strips, which represent the wave fronts when projected to physical space. The fact that bicharacteristic strips remain smooth in phase space in spite of multi-valued wave fronts addresses the difficulties of multi-valuedness. Furthermore, an Eulerian method employing a fixed grid in phase space can be used to capture desired bicharacteristic strips and hence desired wave fronts. This grid handles the problem of resolution. The Eulerian approach adopted in [47] involves the vector valued level set method [8] for representing the high codimensional bicharacteristic strips and solving the Liouville PDE to capture their evolution. We follow the basic framework set in [47] and comment on changes that need to be made specific to our Schrödinger equation setting.

Let $\phi(t, x, p)$ denote the vector valued level set function that represents the bicharacteristic strips in phase space $(x, p) \in \mathsf{IR}^4$. In the two dimensional physical space case, phase space is four dimensional and the bicharacteristic strips, which have the same dimension as the wave fronts, are one dimensional. Following the procedure outlined in [8], a vector valued function ϕ over phase space with three components, $\phi_i, i = 1, 2, 3$, is used to represent the bicharacteristic strips, i.e., they are determined by the set of points where $\phi = 0$, the zero level set.

The Liouville equation (1.6) governs the evolution of the bicharacteristic strips in $(x, p) \in \mathsf{IR}^4$, and thus the wave fronts. This PDE is a transport equation whose velocity field $U(x, p)$ comes from the directions derived in the method of characteristics on our Hamilton-Jacobi equation of interest. In the level set framework we are adopting, the evolution is translated to evolution of the level set function through the Liouville PDE on the components,

$$\partial_t \phi_i + U \cdot \nabla_{\{x,p\}} \phi_i = 0,$$

for $i = 1, 2, 3$. Note each of these equations can be considered independently. The initial ϕ, which we denote by ϕ_0, of course represents the bicharacteristic strips of the initial given wave fronts, usually certain level set curves of the phase. Construction of this function can be easily accomplished. For example, if $\tilde{\phi}_0(x) = S_0(x) - C$ is the level set function

over spatial space that represents the initial given wave fronts, then ϕ_0 is determined through satisfying two conditions. One is that the projection of the zero level set of ϕ_0 to physical space equals the zero level set of $\tilde{\phi}_0$, i.e., the initial wave fronts. This can be accomplished by setting the first component $(\phi_0)_1(x,p) = \tilde{\phi}_0(x)$. The second condition is that $p = \nabla_x S_0$ must be satisfied at the zero level set of ϕ_0, where S_0 is the initial given phase. This can be accomplished by setting the rest of the components as

$$(\phi_0)_i(x,p) = p_{i-1} - (S_0)_{x_{i-1}}(x),$$

for $i = 2, 3$. The evolution PDE's can then be solved with this initial condition in four dimensional phase space to capture the desired bicharacteristic strips and hence the desired wave fronts.

In geometrical optics, the phase S on the wave fronts remains constant during evolution, however, this is not the case in the Schrödinger equation setting. Thus, the phase needs also to be captured so as not to lose important information in the transfer from the linear Schrödinger equation to the Hamilton-Jacobi form. This can be accomplished by solving the Liouville PDE with forcing term,

$$\partial_t S + U \cdot \nabla_{\{x,p\}} S = p \cdot \nabla_p H - H, \tag{4.1}$$

for $S(t,x,p)$ in phase space. The initial condition here is $S(0,x,p) = S_0(x)$. We can thus realize the phase value in the entire domain and, especially, the phase on the bicharacteristic strips can be extracted by looking at S on the zero level set of ϕ. Note that S can be multi-valued when considered in the physical domain. As remarked before, solving the above linearly forced hyperbolic equation is equivalent to solving the level set equation we introduced in §2 in light of "unfolding" the multi-valuedness in (x,p) space. Numerically we choose to solve (4.1) directly and then extract the phase value on the front surface. However in the 1-D setting we use the level set approach to realize the phase value in the whole physical domain, as stated at the end of §3.

The PDE evolution equations for evolution of the bicharacteristic strips and the associated phase can be solved numerically by using explicit finite difference methods over a uniform grid in phase space. The forcing function in the equation for phase can be determined analytically or approximated using central differencing on derivatives. The rest of the terms in all the PDE's look the same and can be discretized using high order upwind schemes for the derivatives in phase space and high order Runge-Kutta methods for the time derivative. We use WENO-Godunov of fifth order [36] and SSP-RK of fourth order [57] or TVD-RK of third order [50] in our simulations. The CFL stability condition in this case says that the time step Δt needs to satisfy

$$\Delta t < \frac{\Delta x}{2 \max_{x,p} |U|},$$

a relatively mild condition on the time step. Note that phase space can be reduced one dimension by replacing p by its angle θ as stated in §3. Such techniques have been successfully used in the geometrical optics case but cannot easily be performed for the problem we are studying since singularities may develop in the evolution equations when $p \cdot \nabla_p H - H = 0$. As the locations of these singularities are not known a priori, we resign ourselves to the full phase space formulation.

In spite of this, we do not, however, need to perform all our calculations at every point of the four dimensional phase space. This is because only the zero level set of ϕ is of interest. Thus it is possible to work in a thin tube surrounding the zero level set, ignoring points far away. This is the main idea behind the local level set method [51], which was implemented successfully for the framework in geometrical optics in [47]. Despite the higher dimension involved in our setting here, the same techniques can be applied to localize around the bicharacteristic strips, working just in a tube of radius proportional to the phase space step size Δx, thus producing an efficient algorithm for wave front construction. We have not yet produced such an algorithm, and thus all our simulations occur over coarse grids in four dimensional phase space, but it is clearly doable. In fact, recent conversations with Chohong Min reveal that a local level set algorithm for vector valued level set functions in arbitrary dimensions may soon be available.

In the local level set approach, reinitialization, i.e., replacement of the nonunique level set functions by better versions, is needed to prevent inaccuracies at the tube boundary from affecting the core, the zero level set. However, reinitialization is also needed to prevent the zero level set surfaces of the components from becoming near parallel to each other at their intersection. This is particularly important when using coarse grids in certain situations, as results in our simulations show. The reintialization algorithm in our work here should differ from that in [47] and those previously investigated since we are dealing with a three component level set function. The desired form for the components are that each is a signed distance function with orthogonal zero level set surfaces. However, in practice, we only need approximations of these properties near the zero level set of the vector valued level set function. In fact, coarse approximations are acceptable in many situations. In this direction, we have implemented numerous ad hoc but fast methods in our studies. A better approach seems to be to evolve the first level set function so that its zero level set, when viewed on the zero level set surface of the second function, is orthogonal to the zero level set of the third function on that surface. This can be accomplished through techniques found in [13]. Then the zero level sets of the first and third can be made orthogonal to that of the second by using the techniques of [8, 47]. Signed distance of the level set functions should be enforced between these steps for a better form. This procedure can be iterated until a desired, numerically more robust form near the bicharacteristic strips is achieved. However, a more careful study of the behavior in general situations is needed.

After the evolution equations are solved to the desired time, the desired wave fronts can be plotted to show the results of the simulation. The high dimension of the phase space considered here, however, complicates matters. At this moment, our simplistic approach to plotting the zero level set of ϕ involves starting with grid points neighboring it. This is already an approximation of the desired bicharacteristic strips, albeit a rough one. The criterion we use to determine if a point neighbors the zero level set is to see if all the components $\phi_i, i = 1, 2, 3$, have different sign at neighboring points. The approximation of the bicharacteristic strips can then be sharpened by considering for each point its projection onto the zero level set surfaces of each of the level set function components, looking at the intersection of the tangent planes there, and replacing the original approximating point by, for example, the closest point in this intersection. Normals of the level set surfaces of

$\phi_i, i = 1, 2, 3$, written as

$$\frac{\nabla \phi_i}{|\nabla \phi_i|},$$

are used for projecting and finding tangent planes. This process can be repeated to satisfaction. Note flowing the original approximating points to satisfy $\sqrt{\phi_1^2 + \phi_2^2 + \phi_3^2} = 1$, as done in [47], can also be employed. The final result is a set of points that approximately lie on the zero level set of ϕ. These points can then be projected to spatial space to form the wave front of interest. Better plotting schemes that produce curves approximating the wave fronts rather than a cloud of points can be found in the recent work of [45].

We now discuss the numerical treatment when construction of the wave fronts and realizing the phase value thereon, in reduced space, is a better choice.

In the phase space $(x, \theta, z) \in \mathsf{IR}^4$ we denote a curve as an intersection of three level set functions ϕ_i for $i = 1, 2, 3$. Thus the system of evolution equations for the time dependent level set functions can be written as

$$\partial_t \phi_i + U(x, \theta, z, \psi) \cdot \nabla_{\{x,\theta,z\}} \phi_i = 0, i = 1, 2, 3,$$

where the Lagrangian index evolves according to

$$\partial_t \psi + U(x, \theta, z, \psi) \cdot \nabla_{\{x,\theta,z\}} \psi = 0,$$

with velocity field U given in (3.4)-(3.7). The role of the z variable is to realize the phase value S on the wave front.

Hence the problem of constructing wave fronts and realizing the phase value becomes one of solving a system of PDE's in IR^4.

In addition to the techniques described above for working in the full phase space, we comment on the choice of initial data and prediction of the Lagrangian index ψ.

It is necessary to initialize the three level set functions to represent a given curve in IR^4. For a given initial curve, we may represent it by constructing level set functions based on the following guiding principles.

(1) One level set gives the initial given front when projected onto physical space;
(2) Another level set is chosen to take care of the angle of the curves;
(3) The last one is chosen to take care of the graph of the initial phase.

One choice for the initial level set $(\phi_{10}, \phi_{20}, \phi_{30})$ is to take

$$\begin{aligned}
\phi_1 &= \phi_0(x), \\
\phi_2 &= \phi_{0x_1} sin\theta - \phi_{0x_2} cos\theta, \\
\phi_3 &= z - S_0(x).
\end{aligned}$$

We should point out when we use the level set method introduced in §2 to resolve the phase value S in the entire domain, we do need to work in the space of $(x, p, z) \in \mathsf{IR}^5$. In the reduced space we also need to predict the Lagrangian index ψ via solving a nonlinear transport equation

$$\partial_t \psi + U(x, \theta, \psi) \cdot \nabla \psi = 0.$$

In the evolution step, one may just use upwind type methods. Initial data needs to be properly chosen. As described above, the initial data of ψ is the parameter of the initial

curve $\phi_0(x) = 0$. One needs to express this parameter in terms of the variables (x, θ, z) in reduced phase space. Let this curve be parameterized as

$$x_1 = x_1(s), \quad x_2 = x_2(s).$$

Then the initial level set $\phi_1 = 0$ leads to

$$\phi_{0x_1}\frac{dx_1}{ds} + \phi_{0x_2}\frac{dx_2}{ds} = 0.$$

From this and the second initial level set $\phi_2 = 0$ we find that

$$g(s) := -\frac{dx_1}{ds}/\frac{dx_2}{ds} = \frac{\phi_{0x_2}}{\phi_{0x_1}} = tan(\theta).$$

Therefore if g is invertible, we have

$$s = g^{-1}(tg(\theta)).$$

This can be done at least for convex curves, see the following illustrative example.

Example. A level curve of an ellipse $\phi_0(x) = \frac{x_1^2}{a^2} + \frac{x_2^2}{b^2} - 1$ can be parameterized as

$$x = acos(s), \quad y = bsin(s), \quad -\pi \le s \le \pi.$$

The corresponding function g is determined by $g = -\frac{dx_1}{ds}/\frac{dx_2}{ds} = \frac{a}{b}tan(s)$ Therefore $s = tg^{-1}[\frac{b}{a}tg(\theta)]$. For a circle, i.e., $a = b$ it turns into $s = \theta$.

5. Numerical Examples

We present several computational examples in order to describe different aspects of our approach. We first consider free motion, where $V(x) = 0$. Thus the total energy is just the kinetic energy

$$H = H(p) = \frac{|p|^2}{2}.$$

The associated Hamiltonian flow is given by $x = \alpha + p_0 t$ and the velocity $p = p_0$ remains constant. We consider examples of phase motion subject to different types of initial phases $S_0(x)$.

Example 1. (No caustics) $S_0(x) = \frac{|x|^2}{2}, \quad x \in \mathsf{IR}^2$

We take as the initial wavefront one of the circles that make up the level sets of $S_0(x)$. The velocity field in Liouville's equation in this case takes the form

$$U(x, p) = (p, 0)$$

and the circle grows.

Figure 1 shows the growth without any added reinitialization. In this case, the zero level sets of the components of the vector valued level set function become close to parallel at a later time and hence the plotter fails to produce a stable curve. Figure 2 shows the same growth with reinitialization. This provides a more desirable level set representation that the plotter can handle. There is no multi-valuedness in this example.

In fact solving the characteristic equation $\frac{d}{dt}(x, p) = (p, 0)$ with initial data $(\alpha, \nabla S_0(\alpha)) = (\alpha, \alpha)$ one gets $x = \alpha(1 + t)$. From $\frac{d}{dt}S = \frac{|p|^2}{2}$ one has $S = S_0(\alpha) + \frac{|p_0|^2}{2}t = \frac{|x|^2}{2(1+t)}$.

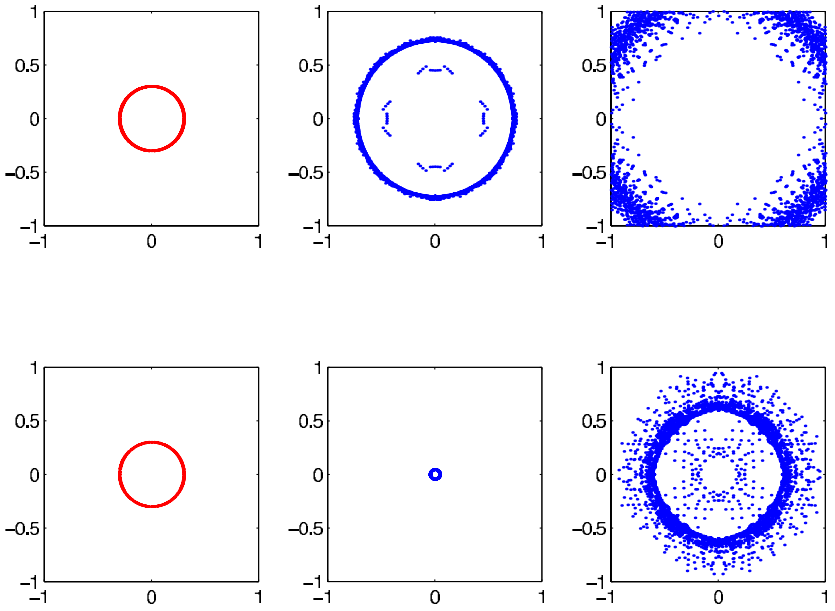

FIGURE 1. The first row shows the effects of a growing circle under free motion when no reinitialization is employed. The second row shows the effects of a shrinking circle in the same setting.

Example 2. (Focus) $S_0(x) = -\frac{|x|^2}{2} \quad x \in \mathbb{R}^2$

In this case, the initial circular wavefront shrinks under the same Liouville equation. Figure 1 once again shows the results with no added reinitialization and figure 3 shows the fixed results when reinitialization is used. Multi-valuedness occurs in this example when the circle becomes a point and then subsequently grows into a circle.

The next series of examples we consider is on the harmonic oscillator. In this case, $V(x) = \frac{|x|^2}{2}$ and so

$$H(x,p) = \frac{|x|^2}{2} + \frac{|p|^2}{2}, \quad x, \quad p \in \mathbb{R}^2.$$

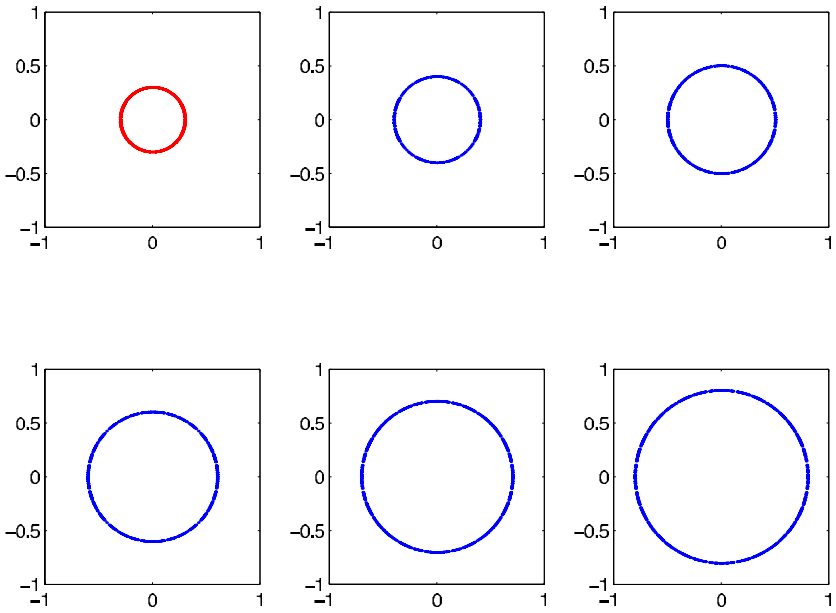

FIGURE 2. The evolution of a growing circle under free motion. Reinitization fixes the problems seen in figure 1.

In this case the Hamiltonian flow is given by

$$x = \alpha cos(t) + p_0 sin(t),$$
$$p = -\alpha sin(t) + p_0 cos(t).$$

Example 3. $S_0(x) = \frac{|x|^2}{2}$. The initial wavefront is once again a circle. The velocity field for the Liouville equation is

$$U(x, p) = (p, -x).$$

In this case, reinitialization is not needed, at least when the chosen final time is not too large.

Figure 4 shows the oscillating nature of the circle in this setting. Multi-valuedness occurs when the circle shrinks to a single point and then expands out again. Actually if the initial wave front is a circle, then the moving wave front is also a circle with oscillating radius, i.e., $|x|^2 = 1 + sin(2t)$.

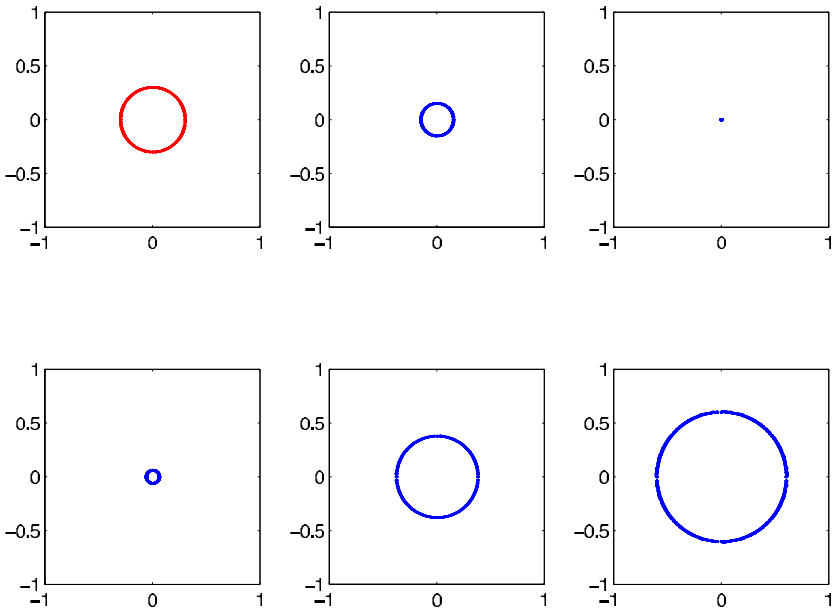

FIGURE 3. The evolution of a shrinking circle under free motion. Reinitization fixes the problems seen in figure 1. Multi-valuedness occurs in this evolution.

Example 4. We collect here results for different initial phases that lead to initial wavefronts of a shifted circle in figure 5 and two circles in figure 6. Note that mult-valuedness occurs both when the circles collapse to a point and, in the case of two circles, when two wavefronts pass through each other.

Finally, figure 7 shows the evolution of an initial wavefront that is a horizontally elongated ellipse and the values of the phase, plotted in the vertical direction, computed for the wavefronts at different times.

Example 5. We consider in this example the case of

$$V(x) = \frac{1}{2}(x_1^2 + \omega x_2^2),$$

for some constant $\omega > 0$. Results are shown in figure 8, with phase in figure 9, when considering an initial elliptical wavefront. Multi-valuedness occurs during the evolution and is successfully dealt with using our approach. Such non-isotropic potential appears,

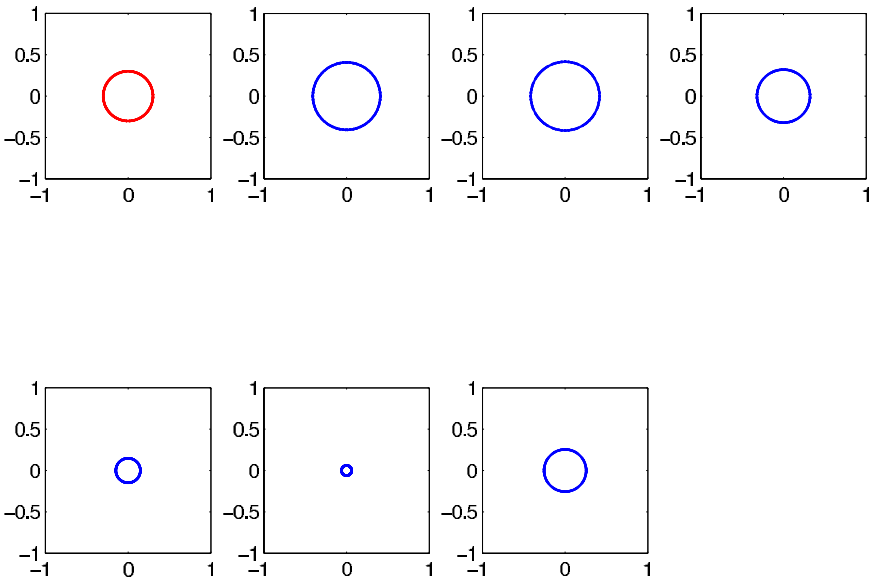

FIGURE 4. An oscillating circle in the harmonic oscillator setting. Note multi-valuedness occurs when the circle collapses to a point.

among others, in the context of Bose-Einstein condenste, in which the trapped potential has different frequencies in the x_1 and x_2 directions, respectively, see e.g. [1].

Example 6. Finally, we consider a different computation of the phase solution in the space (x, p, z), where $x, p, z \in \mathbb{R}$. The initial phase is given by $z = -\ln\cosh x$ in the case of free motion. Level set functions $\psi_1 = z + \ln\cosh x, \psi_2 = p + \partial_x(\ln\cosh x)$ are used to represent the codimension object of interest. Evolution follows the velocity field $(p, 0, -\frac{p^2}{2})$ in the space and thus the curve motion can be captured by solving a transport equation. Results of this computation, with the curve projected into (x, z) space, are shown in figures 10 and 11. We note that a caustic appears and its time and location of appearance agree with the theoretical predictions of $t = 1, x = 0$. Figure 12 shows the results when the projection is made into (x, p) space and figure 13 shows the actual smooth curve evolved in the full (x, p, z) space.

ACKNOWLEDGMENTS

Authors thank two referees who provided valuable comments resulting in improvements in this paper. Cheng's research was supported in part by NSF grant #0208449, Liu's research was supported in part by the National Science Foundation under Grant DMS01-07917, and Osher's research was supported by AFOSR Grant F49620-01-1-0189. This work was initiated while H. Liu was a CAM Assistant Professor at UCLA (January 2000–July 2002). He thanks the Computational and Applied Mathematics (CAM) group at UCLA for its warm hospitality and stimulating environment.

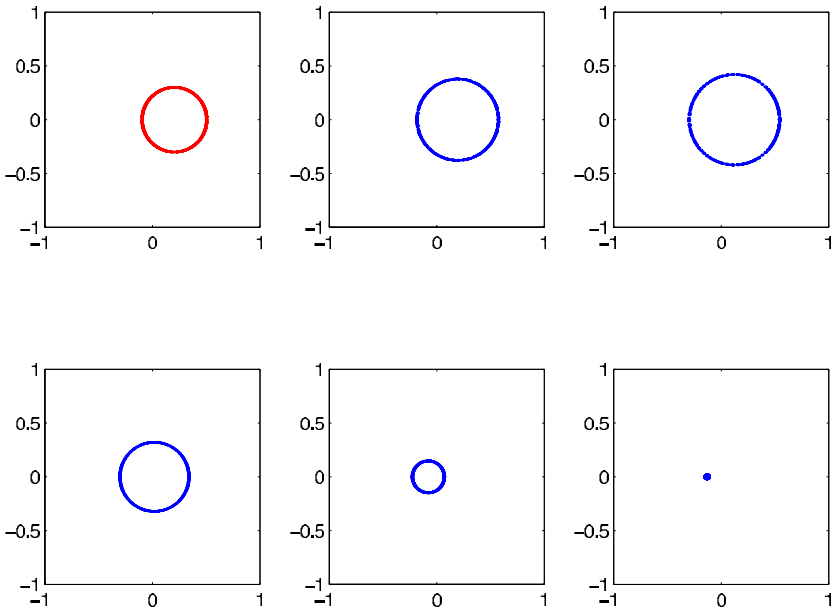

FIGURE 5. An initial circular wavefront not centered at the origin shown in the harmonic oscillator setting. This causes the circle to move left and right while its radius oscillates. Multi-valuedness occurs during the evolution when the circle collapses to a point.

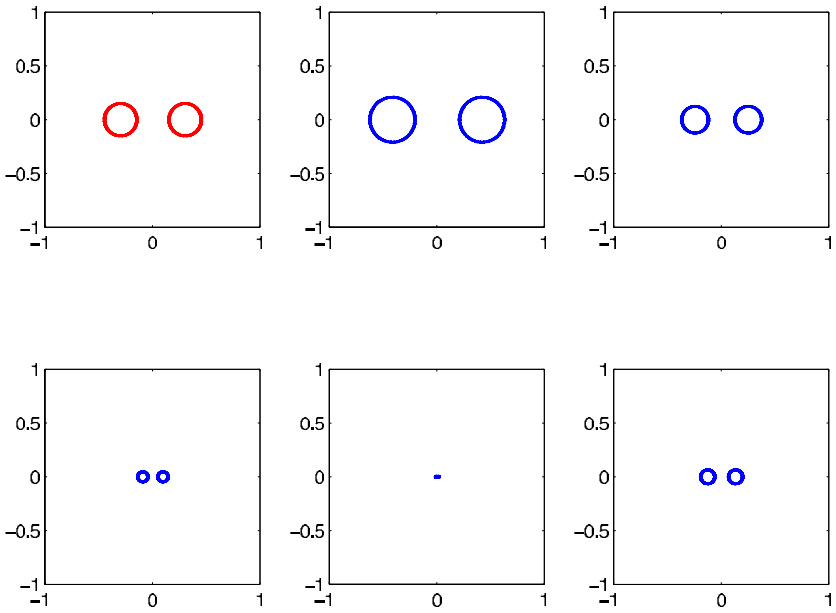

FIGURE 6. Results of the evolution of two initially circlar wavefronts for the harmonic oscillator. In this case, multi-valuedness in addition occurs when the two circles move toward each other and pass through each other while oscillating.

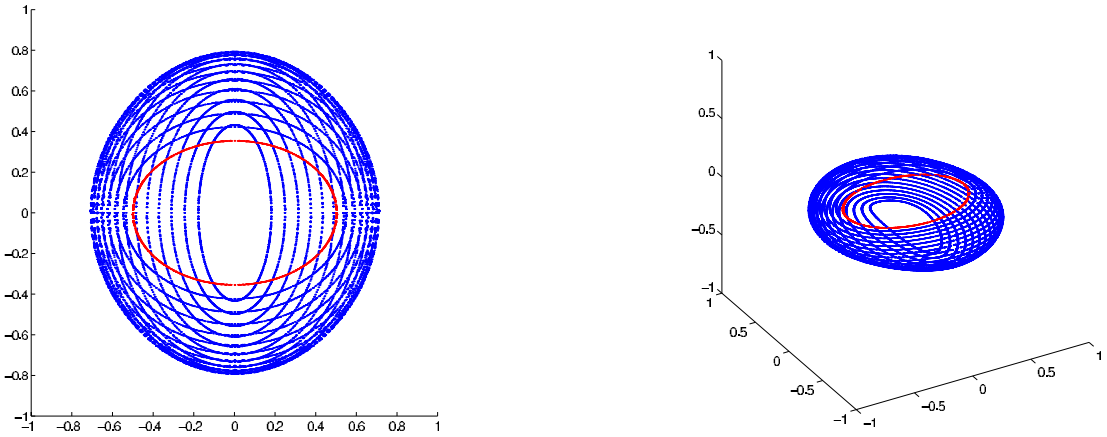

FIGURE 7. In the figure on the left, results of the evolution at different times of an initial horizontally elongated ellipse are plotted in one diagram in the harmonic oscillator setting. The figure on the right shows the corresponding phases on the curves with the vertical direction denoting the value of the phase.

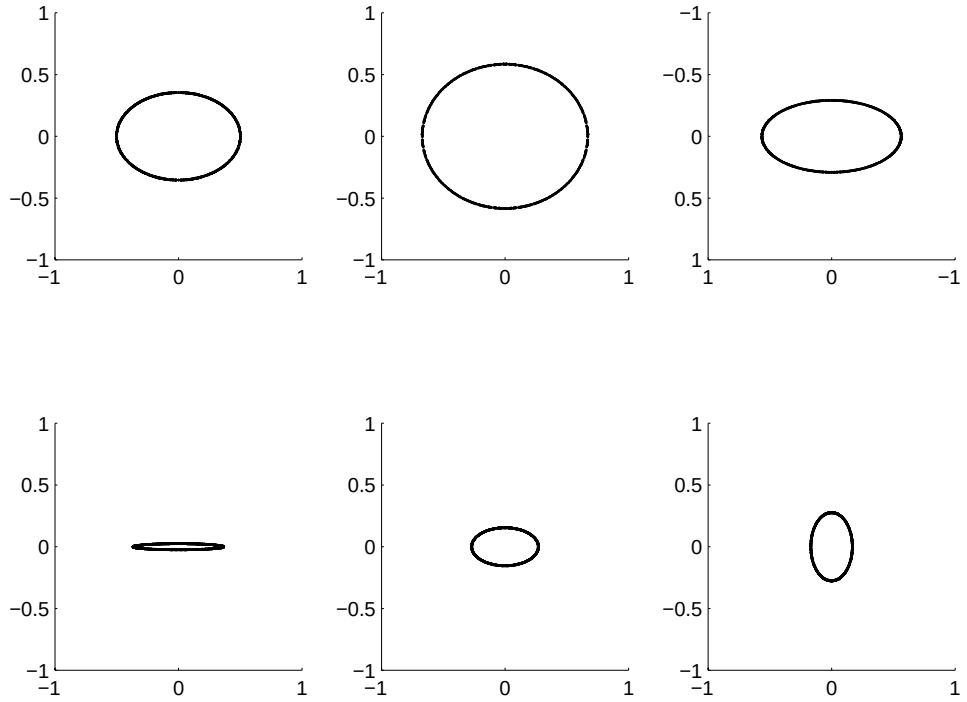

FIGURE 8. An initial elliptical wavefront expands, then contracts, exhibiting multi-valuedness during the flow.

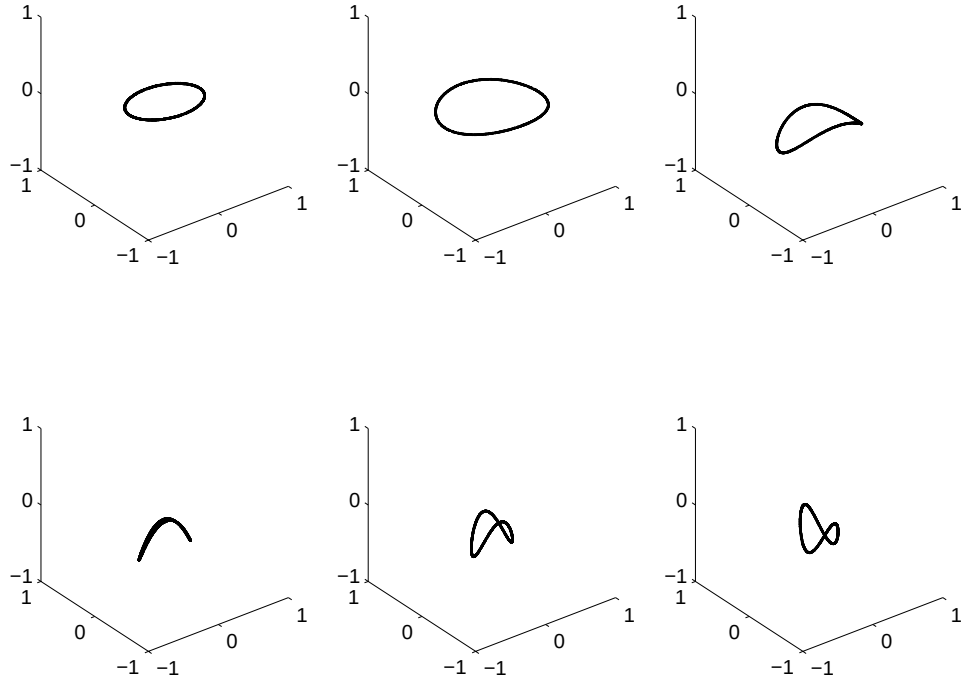

FIGURE 9. The phase values, given by height in vertical direction, on the wavefronts of figure 8.

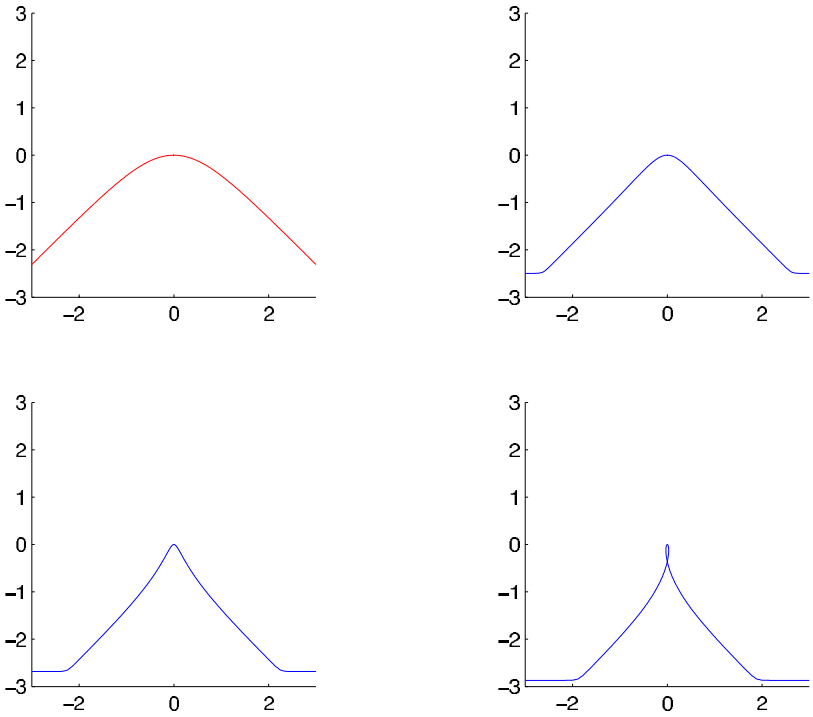

FIGURE 10. Results of phase evolution, with caustic appearing, in free motion. The vertical axis is the phase z and the horizontal axis represents space x. This is projected from (x, p, z) space.

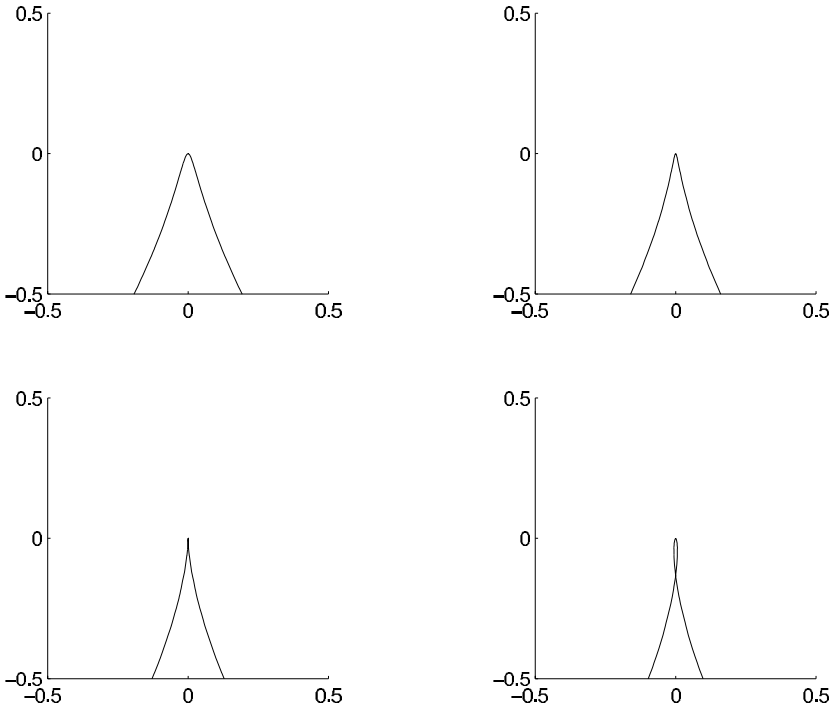

FIGURE 11. A more detailed look at the caustic of the case considered in figure 10. The figures in the top row are a zoomed picture at the area around $x = 0$ immediately before $t = 1$. The figures in the bottom row are the continuation in time showing the caustic immediately after $t = 1$. The location and time of appearance of the caustic agree with theoretical studies.

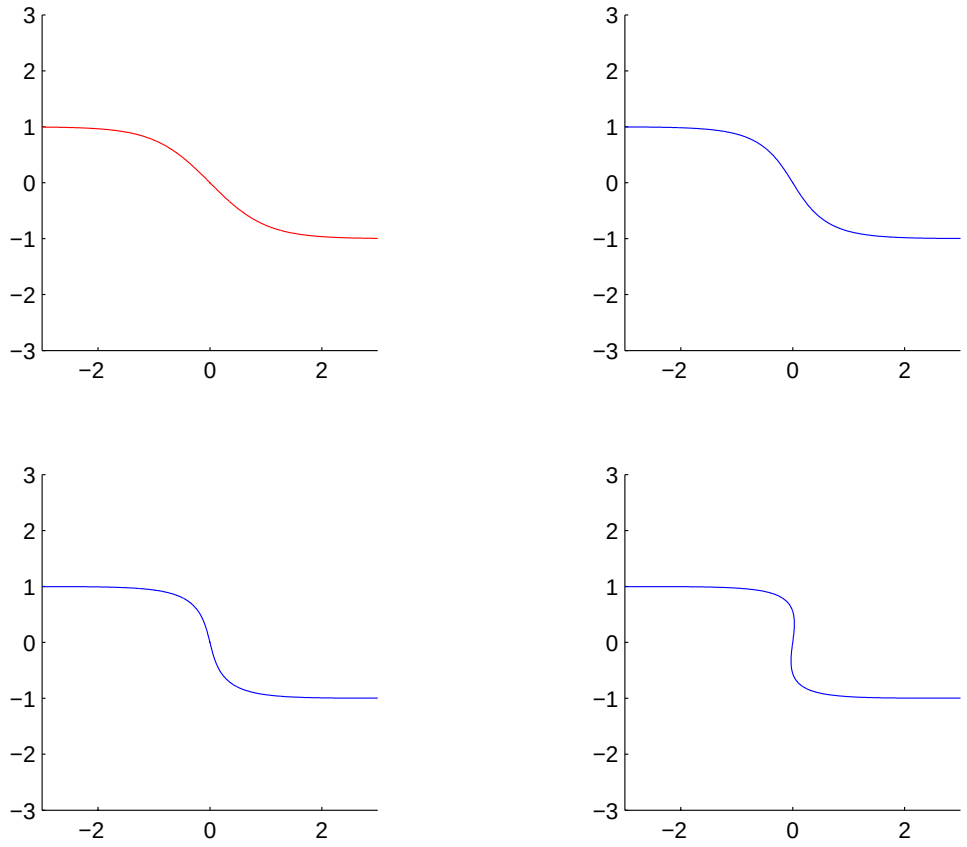

FIGURE 12. Results of the phase evolution of figure 10 from a different viewpoint. In this plot, the vertical axis is p and the horizontal axis is x. This is projected from (x, p, z) space. Note there is no caustic from this viewpoint.

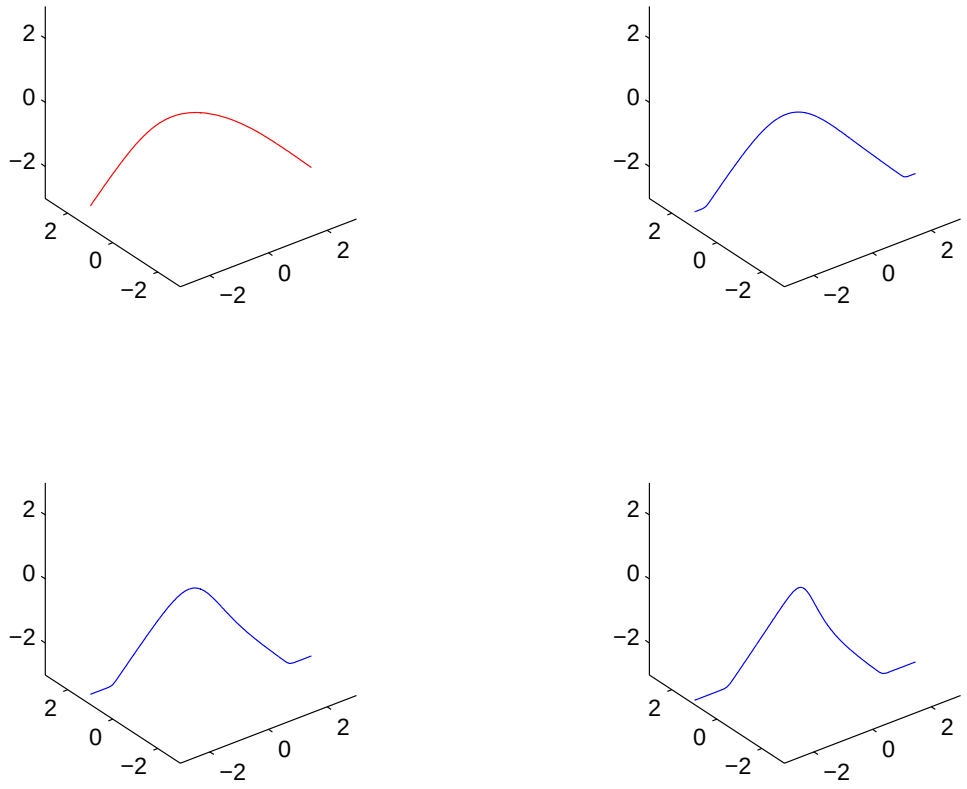

FIGURE 13. The actual curve being evolved in (x, p, z) space in the case considered in figure 10. In this plot, the vertical axis is z and the horizontal axes are x and p. The curve is smooth, but this does not prevent its projection to (x, z) space from having caustics.

References

[1] A. Aftalion and Q. Du, *Vortices in a rotating Bose-Einstein condensate: critical angular velocities and energy diagrams in the Thomas-Fermi regime*, Physics Review A, 2001.

[2] V.M. Babich and N.Y. Kirpichnikova, The Boundary-Layer Method in Diffraction Problems, Springer-Verlag, Berlin-Heidelberg, 1979.

[3] J. D. Benamou, F. Castella, T. Katsaounis and B. Perthame, High-frequency Helmholtz equation, geometrical optics and particle methods, Revist. Math. Iberoam. (2001).

[4] J. D. Benamou, Big ray tracing: Multivalued travel time field computation using viscosity solution of the eikonal equation, *J. Comp. Phys.*, **128** (1996), 463–474.

[5] J. D. Benamou, Direct solution of multivalued phase space solutions for Hamilton-Jacobi equations, *Comm. Pure Appl. math.*, **52** (1999), 1443–1475.

[6] Y. Brenier, Averaged multivalued solutions for scalar conservation laws, SIAM J. Numer. Anal. **21** (1984), 1013–1037.

[7] Y. Brenier and L. Corrias, A kinetic formulation for multi-branch entropy solutions of scalar conservation laws, Ann. Inst. Henri Poincare **15** (1998), 169–190.

[8] P. Burchard and L.-T. Cheng and B. Merriman and S. Osher, Motion of Curves in Three Spatial Dimensions Using a Level Set Approach,J. Comput. Phys., **170**, (2001), 720–741.

[9] F. Bouchut and F. James, Duality solutions for pressureless gases, monotone scalar conservation laws, and uniqueness, *Commun. Partial Diff. Eqs.* **24** (1999), 2173–2189.

[10] R.N. Buchal and J. B. Keller, Boundary layer problems in diffraction theory, Comm. Pure Appl. Math., XIII (1960), 85–114.

[11] G.-Q. Chen and H.-L. Liu, Formation of Delta-Shocks and Vacuum States in the Vanishing Pressure Limit of Solutions to the Isentropic Euler Equations, SIAM J. Math. Anal. **34** (2003), 925–938.

[12] G.-Q. Chen and H.-L. Liu, Concentration and Cavitation in Solutions of the Euler Equations for Nonisentropic Fluids as the Pressure Vanishes, to appear in Phys. D.

[13] L.-T. Cheng and P. Burchard and B. Merriman and S. Osher, Motion of Curves Constrained on Surfaces Using a Level Set Approach,J. Comput. Phys., **175**(2), (2002), 604–644.

[14] L.-T. Cheng and H. L. Liu, *The level set method and Schrödinger equation*, presented at the IPAM workshop on 'Emerging Applications of Nonlinear Schrödinger equations', Feb 6-10, 2003, http://www.ipam.ucla.edu/programs/nls2003/nls2003_schedule.html.

[15] L.-T. Cheng, S. Osher, M. Kang, H. Shim, Y.-H. Tsai, Reflection in a level set framework for geometric optics, Computer Methods in Engineering and Physics, to appear.

[16] R. Courant and D. Hilbert, Methods of Mathematical Physics, Vol 2, New York, Interscience Publishers, 1953-62.

[17] M. Crandall and P.L. Lions, Viscosity solutions of Hamilton-Jacobi equations, Trans. AM. Math. Soc. **282** (1984), 487.

[18] J.J. Duistermaat, Oscillatory integrals, Lagrangian immersions and unfolding of singularities, Comm. Pure Appl. Math. XXVII (1974), 207–281.

[19] W. E, Yu. G. Rykov, and Ya. G. Sinai, Generalized variational principles, global weak solutions and behavior with random initial data for systems of conservation laws arising in adhesion particle dynamics, *Commun. Math. Phys.* **177** (1996), 349–380.

[20] B. Engquist, E. Fatemi and S. Osher, Numerical solution of the high frequency asymptotic expansion for the scalar wave equation, *J. Comput. Phys.*, **120** (1995), 145–155.

[21] B. Engquist and O. Runborg, Computational high frequency wave propagation, Acta Numerica, 2003.

[22] B. Engquist and O. Runborg, Multi-phase computations in geometrical optics, *J. Comp. Appl. Math.*, **74** (1996), 175–1992.

[23] B. Engquist, O. Runborg and T.-K. Tornberg, High frequency wave propagation by the segment projection method, J. Comput. Phys. **178** (2002), 373–390.

[24] L.-C. Evans, A geometric interpretation of the heat equation with multi-valued initial data, SIAM J. Math. Anal. **27** (1996), 932–958.

[25] S. Filippas, G. N. Markrakis, Semiclassical Wigner function and geometrical optics, 2002.

[26] S.M. Flatte, The Schrödinger equation in classical physics, AM.J. Phys., **54** (12) (1986), 1088–1092.
[27] V. Fock, Theory of radion-wave propagation in an inhomogeneous atmosphere for a raised source, Bull. Acad. Sci. USSR, Ser Phys., **14** (1950).
[28] S. Fomel and J.A. Sethian, Fast Phase Space Computation of Multiple Arrivals, LBL,Technical Report, LBNL-48976, (2001).
[29] I. Gasser and P. A. Markowich, Quantum hydrodynamics, Wigner transform and the classical limit, Asymptotic Anal., **14** (1997), 97–116.
[30] L. Gosse, Using K-branch entropy solutions for multivalued geometric optics computations, *J. Comp. Phys.*, **180** (2002), 155–182.
[31] L. Gosse and F. James, Convergence results for inhomogeneous system arising in various high frequency approximations, Numer. Mathmatik, (2001),
[32] L. Gosse, S. Jin and X. Li, On Two Moment Systems for Computing Multiphase Semiclassical Limits of the Schrödinger Equation, preprint, 2003.
[33] L. Gosse and P.A. Markowich, Multiphase semiclassical approximation of an electron in a one-dimensional crystalline lattice, preprint, 2003.
[34] P. Gerard, P. A. Markowich, N. J. Mauser and F. Poupaud, Homogenization limits and Wigner transforms, Comm. Pure Appl. Math., **50** (1997), 323–380.
[35] E. Harabetian and S. Osher, Regularization of ill-posed problems via the level set approach, *SIAM J. Appl. Math.* **58** (1998), 1689–1706.
[36] G.S. Jiang and D. Peng, Weighted ENO Schemes for Hamilton Jacobi Equations, SIAM J. Scient. Comput. **21**, (2000), 2126–2143.
[37] S. Jin and X. Li, Multi-phase computations of the semiclassical limit of the Schrödinger equation and related problems: Whitham Vs Wigner, preprint (2001).
[38] S. Jin and S. Osher, A level set method for the computation of multivalued solutions to quasi-linear hyperbolic PDE's and Hamilton-Jacobi equations, submitted to Comm. Math. Sci.
[39] L. P. Lions and T. Paul, Sur les measures de Wigner, Rev. Math. Iberoamericana, **9** (1993), 563–618.
[40] H.L. Liu, L.-T. Cheng and S. Osher, A level set framework for tracking multivalued solutions to nonlinear first-order equations, 2003.
[41] D. Ludwig, Uniform asymptotic expansions at a caustic, Comm. Pure Appl. Math., XIX (1966), 215–250.
[42] Yu. A. Kravtsov and Yu. I. Orlov, Caustics, Catastrophes and Wave Fields, Springer Series on Wave Phenomena, Springer-Verlag, Berlin, 1993.
[43] S. N. Kružkov, The Cauchy problem in the large for nonlinear equations and for certain quasilinear systems of the first order in several space variables, Soviet Math. Dokl. **5** (1964), 493.
[44] V. P. Maslov and V. M. Fedoryuk, Semi-classical approximation in quantum mechanics, D. Reidel, Dordrecht, 1981.
[45] C. Min, An algorithm constructing the level set in arbitrary dimension and codimension, UCLA CAM Report 03-07, (2003), J. Comput. Phys. (submitted).
[46] S. Osher, *A level set formulation for the solution of the Dirichlet problem for Hamilton-Jacobi equations*, SIAM J. Math. Anal. **24** (1993), 1145–1152.
[47] S. Osher, L.-T. Cheng, M. Kang, H. Shim, Y.-H. Tsai, Geometric Optics in a Phase Space Based Level Set and Eulerian Framework, J. Comput. Phys. **179** (2002), 622–648.
[48] S. Osher and R. Fedkiw, *Level set method and dynamic implicit surfaces*, Springer-Verlag, NY 2002.
[49] S. Osher and J. Sethian, *Fronts propagating with curvature dependent speed: algorithms based on Hamilton-Jacobi formulations*, J. Comput. Phys. **79**, (1988) 12–49.
[50] S. Osher and C.-W. Shu, High order essentially non-oscillatory schemes for Hamilton-Jacobi equations, SINUM, **28** (1991) 907–922.
[51] D. Peng and B. Merriman and S. Osher and H.K. Zhao and M. Kang, A PDE-Based Fast Local Level Set Method, J. Comput. Phys., **155** (1999) 410–438.
[52] J. Qian, L.-T. Cheng and S. Osher, *A level set based Eulerian approach for anisotropic wave propagation*, Wave Motion **37** (2003), 365–379.
[53] O. Runborg, Some new results in multi-phase geometric optics, *Math. Model. Num. Anal.* , **34** (2000), 1203–1231.

[54] H. Sato and M.C. Fehler, Seismic Wave propagation and scattering in the heterogeneous earth, Springer, New York, 1998.
[55] W. Sheng and T. Zhang, *The Riemann Problem for the Transport Equations in Gas Dynamics*, Mem. Amer. Soc. **654** (1999), AMS: Providence.
[56] C. Sparber, P.A. Markowich and N. J. Mauser, *Multivalued Geometrical Optics: Wigner Functions versus WKB-Methods*, preprint, 2001.
[57] R.J. Spiteri and S.J. Ruuth, A New Class of Optimal High-Order Strong-Stability-Preserving Time Discretization Methods, SIAM J. Numer. Anal. **40** (2002), 469–491.
[58] J. Steinhoff, M. Fan and L. Wang, A new Eulerian method for the computation of propagation short acoustic and electromagnetic pulses, *J. Comput. Phys.*, **157** (2000), 683-706.
[59] F.D. Tappert, Diffractive ray tracing of laser beams, J. Opt. SOc. AM., **66**(12) (1976), 1368–1373.
[60] F.D. Tappert, Wave propagation and underwater acoustics (Eds. J. B. Keller and J. S. Papadakis) Lecture Notes in Physics, VOl. 70, Springer, Berlin, 1977.
[61] V.I. Tatarsysii, The effects of the turbulent atmosphere on wave propagation, Israel Program for scientific for Scientific Translation, Jerusalem, 1971.
[62] Y.-H. R. Tsai, Y. Giga and S. Osher, *A level set approach for computating discontinuous solutions of Hamilton-Jacobi equations*, Math. Comp. **72** (2003), 159–181.
[63] B. R. Vainberg, Asymptotic Methods in Equations of Mathematical Physics, Gordon and Breach, New York, 1989.

UC San Diego, Mathematics Department, La Jolla, CA 92093-0112
E-mail address: lcheng@math.ucsd.edu

UCLA, Mathematics Department, Los Angeles, CA 90095-1555.
Current address: Iowa State University, Mathematics Department, Ames, IA 50011
E-mail address: hliu@iastate.edu

Level Set Systems, Inc, 1058 Embury Street, Pacific Palisades, CA 90272-2501
E-mail address: sjo@levelset.com